A Theoretical Study of Free and $Fe(CO)_4$-Complexed Borylenes (Boranediyls) and Heavier Congeners: The Nature of the Iron−Group 13 Element Bonding

Charles L. B. Macdonald and Alan H. Cowley*

Contribution from the Department of Chemistry and Biochemistry, The University of Texas at Austin, Austin, Texas 78712

Received July 20, 1999

Abstract: The singlet and lowest-lying triplet states of the univalent group 13 ligands MeM, (η^5-C_5H_5)M, (η^5-C_5Me_5)M, and $(H_3Si)_2NM$ (M = B, Al, Ga, In) have been investigated by DFT methods. Each ligand possesses a singlet ground state. Four models were considered for the interaction of these ligands with the $Fe(CO)_4$ fragment: a purely M → Fe σ-bonded model (**A**) supplemented by one back-bonding interaction from Fe to M (**B**), or a M → Fe σ-bonded model supplemented by two back-bonding interactions from Fe to M (**C**), and a M═Fe double-bonded model (**D**). In general, the DFT calculations indicated that the RM ligands behave as two-electron donors (i.e. bonding model **A**). The RM ligands with non π-bonding substitutents, R, were found to have some π-acceptor capability that would be appropriate for iron → ligand back-bonding. However, evidence for such an interaction was only found in the case of $MeBFe(CO)_4$.

Introduction

Starting with pioneering work on the ligative possibilities of boron monofluoride,[1] interest in transition metal complexes that feature η^1-bonding of group 13 fragments of the type RM (M = B, Al, Ga, and In) has grown steadily.[2] An early example of such a complex, (bipy)$EtGaFe(CO)_4$ (bipy = bipyridyl), involves bidentate Lewis base stabilization of the terminally bound EtGa (gallanediyl) moiety.[3] Although the complex was not characterized structurally, it was shown to be monomeric in solution. Support for the proposed structure was provided by a more recent X-ray structural analysis of the related complex, [(tmeda)-$MeGaCr(CO)_5$] (tmeda = *N*,*N*,*N*′,*N*′-tetramethylethylenediamine).[4] The first structurally authenticated examples of terminally bonded indanediyls were the pyrazolylborate complexes $HB(3,5\text{-}Me_2pz)_3InFe(CO)_4$ and $HB(3,5\text{-}Me_2pz)_3InW(CO)_5$.[5] Complexes free of external Lewis bases have been obtained by the use of sterically demanding substituents on the group 13 element. Thus, $((Me_3Si)_3CIn)_4Ni$,[6] (Trip)$GaFe(CO)_4$[7] (Trip = 2,6-bis(2,4,6-triisopropylphenyl), (Trip)$InMn(\eta^5\text{-}C_5H_5)(CO)_2$,[8] ($\eta^5$-$C_5Me_5$)$GaFe(CO)_4$,[9] and ($\eta^5$-$C_5Me_5$)$MCr(CO)_5$ (M = Al,[10] Ga,[9] In[11]) feature appropriately bulky alkyl, aryl or cyclopentadienyl groups. The C_5Me_5 substituent has also proved to be effective for the isolation and X-ray structural assay of (η^5-C_5Me_5)$AlFe(CO)_4$ and (η^5-C_5Me_5)$BFe(CO)_4$, the first examples of terminal alanediyl[12] and boranediyl[13] complexes, respectively. In a subsequent development, it was shown that the bulky amido ligand, $(Me_3Si)_2N$, can also be used for the isolation of the boranediyl complexes of the type $(Me_3Si)_2NBM(CO)_6$ (M = Cr, W).[14]

Interest in compounds with group 13-transition metal bonds has been generated for both practical and theoretical reasons. Regarding the former, such compounds are potentially useful as single-source chemical vapor deposition (CVD) sources to important intermetallic phases such as β-CoGa and ϵ-NiIn.[15] From the electronic structural standpoint, considerable discussion has arisen recently regarding the nature of the bonding between the group 13 element and the transition metal[7,10,13,14,16−19] Four bonding models, **A**−**D**, can be considered for the covalent

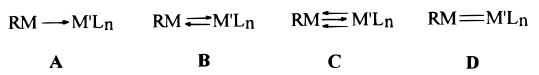

interaction between group 13 (RM) and transition metal ($M'L_n$)

(1) Timms, P. L. *Acc. Chem. Res.* **1973**, *6*, 118.
(2) For recent discussions, see (a) Wrackmeyer, B. *Angew. Chem., Int. Ed.* **1999**, *38*, 771. (b) Murugavel, R.; Chandrasekhar, V. *Angew. Chem., Int. Ed.* **1999**, *38*, 1211.
(3) Cymbaluk, T. H.; Ernst, R. D. *Inorg. Chem.* **1980**, *19*, 2381.
(4) Schulte, M. M.; Herdtweck, E.; Randaschl-Sieber, G.; Fischer, R. A. *Angew. Chem., Int. Ed. Engl.* **1996**, *35*, 424.
(5) (a) Reger, D. L.; Mason, S. S.; Rheingold, A. L.; Haggerty, B. S.; Arnold, F. P. *Organometallics* **1994**, *13*, 5049. (b) Reger, D. L. *Coord. Chem. Rev.* **1996**, *147*, 571.
(6) Uhl, W.; Pohlmann, M.; Warchow, R. *Angew. Chem., Int. Ed.* **1998**, *37*, 961.
(7) Su, J.; Li, X.-W.; Crittendon, R. C.; Campana, C. F.; Robinson, G. H. *Organometallics* **1997**, *16*, 4511.
(8) Haubrich, S. T.; Power, P. P. *J. Am. Chem. Soc.* **1998**, *120*, 2202.
(9) Jutzi, P.; Neumann, B.; Reumann, G.; Stammler, H.-G. *Organometallics* **1998**, *17*, 1305.
(10) Yu, Q.; Purath, A.; Donchev, A.; Schnöckel, H. *J. Organomet. Chem.* **1999**, *584*, 94.
(11) Jutzi, P.; Neumann, B.; Reumann, G.; Schebaum, L. O.; Stammler, H.-G. *Organometallics* **1999**, *18*, 2550.
(12) Weiss, J.; Stetzkamp, D.; Nuber, B.; Fischer, R. A.; Boehme, C.; Frenking, G. *Angew. Chem., Int. Ed. Engl.* **1997**, *36*, 70.
(13) Cowley, A. H.; Lomeli, V.; Voigt, A. *J. Am. Chem. Soc.* **1998**, *120*, 6401.
(14) Braunschweig, H.; Kollan, C.; Englert, U. *Angew. Chem., Int. Ed.* **1998**, *37*, 3179.
(15) See, for example, (a) Chen, Y.-J.; Kaesz, H. D.; Kim, Y. K.; Müller, H. J.; Williams, R. S.; Yue, R. S. *Appl. Phys. Lett.* **1989**, *55*, 2760. (b) Fischer, R. A.; Behm, J.; Priermeier, T.; Scherer, W. *Angew. Chem., Int. Ed. Engl.* **1993**, *32*, 746. (c) Fischer, R. A.; Scherer, W.; Kleine, M. *Angew. Chem., Int. Ed. Engl.* **1993**, *32*, 748. (d) Maury, F.; Brandt, L.; Kaesz, H. D. *J. Organomet. Chem.* **1993**, *449*, 159. (e) Fischer, R. A.; Miehr, A.; Schulte, M.; Hardtweck, E. *J. Chem. Soc., Chem. Commun.* **1995**, 337.
(16) Driess, M.; Grützmacher, H. *Angew. Chem., Int. Ed. Engl.* **1996**, *35*, 828.

10.1021/ja992573l CCC: $18.00
Published on Web 12/14/1999

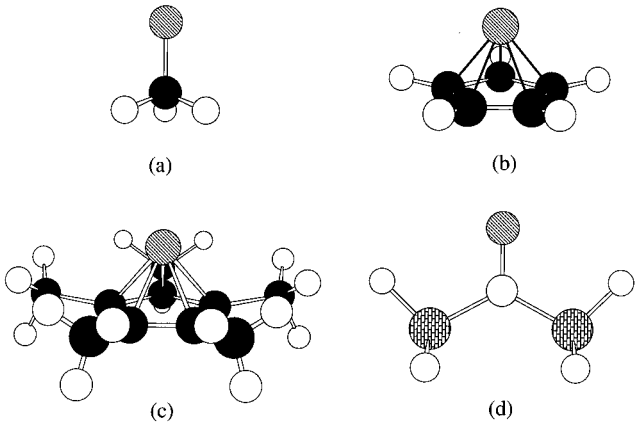

Figure 1. Drawings of representative RM ligands: (a) R = Me, (b) R = (η^5-C_5H_5), (c) R = (η^5-C_5Me_5), (d) R = $(H_3Si)_2N$.

fragments. One of the conspicuous differences between these bonding models relates to the electronic state of the group 13 fragment, RM. Thus, structures **A**, **B**, and **C** imply that the RM moiety coordinates in a singlet state. In structure **A** there is a simple donor−acceptor bond between M and M′, while structures **B** and **C** feature one and two additional back-bonding interactions from the transition metal to the group 13 element, thereby developing double and triple bonds, respectively, between M and M′. The double-bonded structure, **D**, implies that the RM fragment bonds as a triplet state.

The fundamental objective of the present work was to investigate the relative merits of the bonding models that have been proposed for terminal boranediyl and heavier congeneric complexes by means of density functional theory (DFT) calculations. We chose to focus on the model complexes (η^5-C_5H_5)$MFe(CO)_4$ (M = B, Al, Ga, In) primarily because the M = B, Al, and Ga derivatives are all known (albeit with η^5-C_5Me_5 rather than η^5-C_5H_5 substituents) and X-ray crystallographic data available. However, we have also performed DFT calculations on complexes of the type $MeMFe(CO)_4$ (M = B, Al, Ga, In) to determine if these are better candidates for M−Fe multiple bonding. Finally, the amido-substituted boranediyl complex $(H_3Si)_2NBFe(CO)_4$, was investigated at the same level of theory to assess the nature of the B−Fe and N−B bonding in light of the recently reported preparation of $(Me_3Si)_2NBFe(CO)_4$ (and the related, crystallographically confirmed complex, $(Me_3Si)_2NBW(CO)_5$).[14] The model alanediyl complex, (η^5-C_5H_5)$AlFe(CO)_4$, has, in fact, been studied previously by DFT methods[4,20] and the present results are in satisfactory agreement with this earlier work. Other related work in this area includes DFT studies of (aryl)$GaFe(CO)_4$ (aryl = C_6H_5 [17,18] and a series of model boranediyl complexes of the general type $RBM(CO)_n$ (R = F, NH_2, O^-; $M(CO)_n$ = $Cr(CO)_5$, $[Mn(CO)_5]^+$, $Fe(CO)_4$, $[Co(CO)_4]^-$, and $Ni(CO)_3$).[21]

As an integral part of the present DFT study, we have also examined the uncoordinated RM ligands (Figure 1: R = η^5-C_5H_5, (η^5-C_5Me_5)Me, $N(SiH_3)_2$; M = B, Al, Ga, In) to establish their ground states, frontier orbitals, and singlet−triplet energy gaps. Theoretical studies of individual examples of some of these RM ligands have already appeared in the literature, particularly with respect to their oligomerization;[22] however, we are not aware of a previous systematic theoretical investigation of these monovalent Group 13 species.

Theoretical Methods

All DFT calculations were performed using the Gaussian 94[23] suite of programs, Becke's gradient-corrected exchange functional,[24] and Perdew's correlation functional[25] (BP86). Two different basis sets were employed in the present study. All-electron basis sets were used for C, H, O, N, Si (6-31G(d)), and the group 13 elements (6-31+G(d)); Fe was modeled with the quasi-relativistic effective core potential (ECP) and (311111/22111/411) subvalence and valence basis set of Dolg et al.[26] (this overall basis set is designated **A**). The second basis set consisted of the same functions for C, H, O, and Fe; however, the group 13 elements were approximated by the Los Alamos National Laboratory LANL2dz ECP and valence basis set (this overall basis set is designated **B**). The geometry of each molecule was optimized at the BP86/**A** or **B** level of theory and was restricted to the highest reasonable symmetry (C_s for all iron tetracarbonyl complexes). Vibrational frequency analysis was performed on all RM compounds to confirm the nature of the stationary points. This analysis was not performed for any of the iron tetracarbonyl complexes because of the excessive computational cost; however, the computed structures are in close correspondence with the available experimental data which implies that the geometries are of minimum energy. Furthermore, since Ehlers et al.[21] have demonstrated the preference for axial coordination of several RB ligands, the equatorial isomers were not examined. The group 13 element−Fe bonding was examined by NBO[27] and fragment analysis.[28] All calculations were performed on either IBM RS/6000 or SGI Octane workstations. Graphical representations of the calculated molecular orbitals were produced using the Molden[29] program. The total energies of all singlet species are collected in Table 1. The orbitals that are discussed are of the Kohn−Sham type, and their energies have not been corrected in the manner suggested recently by Stowasser and Hoffmann.[30] Note that the electronic properties calculated for (η^5-C_5H_5)-$BFe(CO)_4$ and $MeInFe(CO)_4$ using the LANL2dz potential on M are not reasonable; hence, these particular cases will not be discussed further. GIAO NMR calculations[31] of the ^{11}B chemical shifts were

(17) Cotton, F. A.; Feng, X. *Organometallics* **1998**, *17*, 128.
(18) Boehme, C.; Frenking, G. *Chem. Eur. J.* **1999**, *5*, 2184.
(19) *Chem. Eng. News*, March 16, 1998; p 31 and August 2, 1999; p 23.
(20) Üffing, C.; Ecker, A.; Köppe, R.; Schnöckel, H. *Organometallics* **1998**, *17*, 2373.
(21) Ehlers, A. W.; Baerends, E. J.; Bickelhaupt, F. M.; Radius, R. *Chem. Eur. J.* **1998**, *4*, 210.
(22) See, for example: B: (a) Swanton, D. J.; Ahlrichs, R.; Häser, M. *Chem. Phys. Lett.* **1989**, *155*, 329. (b) Swanton, D. J.; Ahlrichs, R. *Theor. Chim. Acta* **1989**, *75*, 163. Al: (c) Ahlrichs, R.; Ehrig, M.; Horn, H. *Chem. Phys. Lett.* **1991**, *183*, 227. (d) Schneider, U.; Ahlrichs, R.; Horn, H.; Schäfer, A. *Angew. Chem., Int. Ed. Engl.* **1992**, *31*, 353. (e) Gauss, J.; Schneider, U.; Ahlrichs, R.; Dohmeier, C.; Schnöckel, H. *J. Am. Chem. Soc.* **1993**, *115*, 2402. (f) Purath, A.; Dohmeier, C.; Ecker, A.; Schnöckel, H. *Organometallics* **1998**, *17*, 1894. Ga: (g) Loos, D.; Schnöckel, H.; Gauss, J.; Schneider, U. *Angew. Chem., Int. Ed. Engl.* **1992**, *31*, 1362. In: (h) Lattman, M.; Cowley, A. H. *Inorg. Chem.* **1984**, *23*, 241. (i) Janiak, C.; Hoffmann, R. *J. Am. Chem. Soc.* **1990**, *112*, 5924. (j) Budzelzaar, P. H. M.; Boersma, J. *Rec. Trav. Chim. Pays-Bas* **1990**, *109*, 187. (k) Uhl, W.; Jantschak, A.; Saak, W.; Kaupp, M.; Wartchow, R. *Organometallics* **1998**, *17*, 5009.
(23) Frisch, M. J.; Trucks, G. W.; Schlegel, H. B.; Gill, P. M. W.; Johnson, B. G.; Robb, M. A.; Cheeseman, J. R.; Keith, T. A.; Petersson, G. A.; Montgomery, J. A.; Raghavachari, K.; Al-Laham, M. A.; Zakrewski, V. G.; Ortiz, J. V.; Foresman, J. B.; Cioslowski, J.; Stefanow, B. B.; Nanayakkara, A.; Challacombe, M.; Peng, C. Y.; Ayala, P. Y.; Chen, W.; Wong, M. W.; Andres, J. L.; Replogle, E. S.; Gomperts, R.; Martin, R. L.; Fox, D. J.; Binkley, J. S.; DeFrees, D. J.; Baker, J.; Stewart, J. P.; Head-Gordon, M.; Gonzalez, C.; Pople, J. A. *GAUSSIAN 94*, revision B.2; Gaussian, Inc.: Pittsburgh, PA, 1995.
(24) Becke, A. D. *Phys. Rev.* **1988**, *38*, 3098.
(25) Perdew, J. P. *Phys. Rev.* **1986**, *33*, 8822.
(26) Dolg, M.; Wedig, U.; Stoll, H.; Preuss, H. *J. Chem. Phys.* **1987**, *86*, 866.
(27) NBO Version 3.1, E. D. Glendening, A. E. Reed, J. E. Carpenter, and R. Weinhold. See also: Reed, A. E.; Curtiss, L. A.; Weinhold, F. *Chem. Rev.* **1988**, *88*, 899.
(28) Derived from the analysis of Zeigler, et al., see, for example: (a) Ziegler, T.; Rauk, A.; *Theor. Chim Acta* **1977**, *46*, 1. (b) Ziegler, T.; Rauk, A. *Inorg. Chem.* **1992**, *31*, 4864. (d) Jacobsen, H.; Berke, H.; Döring, S.; Kehr. G.; Erker, G.; Fröhlich, R.; Meyer, O. *Organometallics* **1999**, *18*, 1724.
(29) Shaftenaar, G. MOLDEN 3.4; CAOS/CAMM Center Nijmegen: Toernooiveld, Nijmegen, The Netherlands, 1991.
(30) Stowasser, R.; Hoffmann, R. *J. Am. Chem. Soc.* **1999**, *121*, 3414.

Table 1. Calculated Total Energies (au) for All Singlet Species

compound	energy (optimized)	energy (coordinated geometry)	
	MeM Ligands (C_{3v})		
B	−64.627518 (−64.617601)[a]		
Al	−282.305804 (−41.881987)		
Ga	−1962.905232 (−41.955376)		
In	(−41.782456)		
	(η^5-C_5H_5)M Ligands (C_{5v})		
B	−218.257356 (−218.242715)		
Al	−435.960681 (−195.532630)		
Ga	−2116.559523 (−195.607033)		
In	(−195.436325)		
	(η^5-C_5Me_5)M Ligands (C_{5v})		
B	−414.840110 (−414.821614)		
Al	−632.531249 (−392.100151)		
Ga	−2313.129127 (−392.173600)		
In	(−392.000604)		
	($H_3Si)_2$NM Ligands (C_{2v})		
B	−662.164821 (−662.149190)		
Al	−879.832020 (−639.404491)		
Ga	−2560.423817 (−639.476347)		
In	(−639.302820)		
	Iron Carbonyls		
Fe(CO)$_4$ (C_s)	−577.408935		
Fe(CO)$_4$ (C_{3v})	−577.394454		
CO ($C_{\infty v}$)	−113.307691		
Fe(CO)$_5$ (D_{3h})	−690.786275	CO	Fe(CO)$_4$ fragment
		−113.304886	−577.391408

Complexes (C_s)

(η^5-C_5H_5)MFe(CO)$_4$	complex	(η^5-C_5H_5)M ligand	Fe(CO)$_4$ fragment
B	−795.780720 (−793.205371)	−218.250045 (−218.226646)	−577.388456 (−577.388365)
Al	−1013.451566 (−773.013501)	−435.954441(−195.525396)	−577.390009 (−577.391475)
Ga	−2694.027691 (−773.073202)	−2116.553601(−195.599738)	−577.392766 (−577.392708)
In	(−772.895211)	(−195.431368)	(−577.393059)

MeMFe(CO)$_4$	complex	MeM ligand	Fe(CO)$_4$ fragment
B	−642.188746 (−642.183051)	−64.627408 (−64.617074)	−577.387843 (−577.388515)
Al	−859.815288 (−619.386495)	−282.305137 (−41.881083)	−577.389584 (−577.390852)
Ga	−2540.409571 (−619.456673)	−1962.903773 (−41.953584)	−577.391380 (−577.391566)
In	(−619.276740)	(−41.780435)	(−577.391624)

($H_3Si)_2$NMFe(CO)$_4$	complex	($H_3Si)_2$NB ligand	Fe(CO)$_4$ fragment
B	−1239.700528	−662.164491	−577.388944

Miscellaneous Compounds

[MeBH]$^+$ (C_{3v})	−64.999282
[(η^5-C_5H_5)BH]$^+$ (C_{5v})	−218.697603
[($H_3Si)_2$NBH]$^+$ (C_{2v})	−662.554254
F_3BOMe_2 (C_s)	−479.575465

[a] Results for basis set B in parentheses.

performed using the BP86/A level of theory, and the computed chemical shifts are referenced to the chemical shielding of Me_2OBF_3, which was optimized in an identical manner and assumed to have a chemical shift of 0.0 ppm. All contour diagrams have a contour separation of 0.025 au and are scaled identically within a given series. All three-dimensional diagrams are drawn with a cutoff of 0.05 au unless indicated otherwise.

Results and Discussion

1. RM Ligands (R = Me, η^5-C_5H_5, η^5-C_5Me_5, N(SiH$_3$)$_2$; M = B, Al, Ga, In). As pointed out in the Introduction, boranediyls and heavier congeners can bond to transition metal fragments either in the singlet or triplet states. The lowest-energy singlet and triplet states of the Fe(CO)$_4$ fragment are almost equal in energy;[21] thus, at the outset it was important to establish the nature and relative energies of the frontier orbitals of the isolated RM ligands. The first point to note concerning these ligands is that, regardless of the substituent R, the ground state is a singlet in each case (Table 2). Such a conclusion is in accord with a variety of calculations on boranediyls.[21,22] With the exception of the RIn ligands, the singlet−triplet energy gap, ΔE_{S-T}, increases with increasing atomic number of M. Also, note that the singlet−triplet gaps are larger for the π-donating cyclopentadienyl- and amido-substituted ligands than for the methyl analogues. Such a trend has also been observed for carbenes.[16]

In general, there is excellent agreement between the DFT calculated singlet structures and the available experimental structural information. Gas-phase electron diffraction data are available for (η^5-C_5H_5)In[32] and the pentamethylcyclopentadienyl-substituted species, (η^5-C_5Me_5)M (M = Al,[33] Ga,[34] In[35]), and a comparison of these data with the DFT calculated values

(31) Wolinski, K.; Hinton, J. F.; Pulay, P. *J. Am. Chem. Soc.* **1990**, *112*, 8251.

(32) Shibata, S.; Bartell, L. S.; Gavin, R. M., Jr. *J. Chem. Phys.* **1964**, *41*, 717.

Table 2. Triplet Energies (au) and Singlet−Triplet Energy Gaps (kcal/mol) for RM Ligands

ligand	*E* (triplet)	ΔE_{S-T}
	$(C_s)^a$	
MeB	−64.5721302 (−64.569396)[b]	34.65 (30.25)[b]
MeAl	−282.23635 (−41.814549)	43.58 (42.32)
MeGa	−1962.8276 (−41.882593)	48.72 (45.67)
MeIn	(−41.714305)	(42.77)
	$(C_s)^a$	
(η^5-C_5H_5)B	−218.17609 (−218.15795)	50.99 (53.19)
(η^5-C_5H_5)Al	−435.84546 (−195.42046)	72.30 (70.39)
(η^5-C_5H_5)Ga	−2116.4365 (−195.48783)	77.17 (74.80)
(η^5-C_5H_5)In	(−195.32326)	(70.95)
	$(C_s)^a$	
(η^5-C_5Me_5)B	−414.75282 (−414.73484)	53.19 (54.78)
(η^5-C_5Me_5)Al	−632.41829 (−391.99250)	70.89 (67.55)
(η^5-C_5Me_5)Ga	−2313.01790 (−392.06700)	69.81 (66.89)
(η^5-C_5Me_5)In	(−391.90348)	(60.95)
	$(C_{2v})^a$	
$(H_3Si)_2NB$	−662.08384 (−662.07501)	50.82 (46.55)
$(H_3Si)_2NAl$	−879.73391 (−639.3079)	61.56 (60.61)
$(H_3Si)_2NGa$	−2560.3076 (−639.36716)	72.95 (68.52)
$(H_3Si)_2NIn$	(−639.19545)	(67.37)

[a] Molecular symmetry of triplet state. [b] Results for basis set B in parentheses.

is presented in Table 3. As expected, the R−M bond distance increases with the atomic number of M for both the η^5-C_5H_5 and η^5-C_5Me_5 substituents and, in common with many other organoaluminum and organogallium compounds, the C−Al and C−Ga bond distances are almost identical.[36] Note also that the H atoms or Me groups are bent out of the plane of the C_5 ring and toward the group 13 element. This direction of bending is inconsistent with the view[12] that the bonding is ionic, viz. $(C_5R_5)^-M^+$.[37] Unfortunately, no experimental structural data are available for the MeM and $(H_3Si)_2NM$ ligands. As shown in Table 4, the closest compound to MeGa for which gas-phase electron diffraction data are available is the bulky alkylated monomer, $(Me_3Si)_3CGa$, and the calculated and experimental M−C bond distances for these species are in satisfactory agreement. In other cases, comparisons are made with X-ray crystallographic data for oligomeric derivatives.

The coordination behavior of RM ligands can be understood, for the most part, through an examination of the energies and symmetry characteristics the relevant frontier orbitals. At the outset it is important to draw a distinction between the σ-type and π-type molecular orbitals. The HOMO for almost every RM ligand exhibits a distinctly lone pair (σ-type) character as illustrated in Figure 2 for the boranediyls, RB (R = Me, η^5-C_5R_5, $(H_3Si)_2N$). The molecular orbitals are qualitatively very similar for the HOMOs of the heavier congeners; however, the magnitude of the "lone pair" contribution to the wave functions decreases with atomic number. The only exceptions to this generalization are (η^5-C_5R_5)Ga and (η^5-C_5R_5)In for which the HOMO is of e_1 symmetry and corresponds to the π-bonds between the η^5-C_5R_5 fragment and the group 13 element as shown in Figure 3. In the case of (η^5-C_5H_5)M (M = Ga, In) ligands, the e_1 and a_1 orbitals are almost isoenergetic with the a_1 orbital slightly lower in energy [$E(e_1) - E(a_1)$; M = Ga: 4.17 (1.95) kcal/mol; In: (7.25 kcal/mol)]. For the (η^5-C_5Me_5)M ligands the difference in energy increases somewhat [$E(e_1) - E(a_1)$; M = Ga: 12.82 (10.83) kcal/mol; In: (17.47 kcal/mol)]; however, in the coordinated geometry each RM ligand in is found to have a "lone pair" HOMO (vide infra).

Table 3. Calculated and Experimental Metrical Parameters for (η^5-C_5H_5)M and (η^5-C_5Me_5)M Ligands

compound		calculated[a,b]	experimental
(η^5-C_5H_5)B	B−C	1.977 (2.080)[c]	
	C−C	1.424 (1.426)	
	C−H	1.090 (1.090)	
	C_5, C−H[a]	7.71 (6.14)	
(η^5-C_5H_5)Al	Al−C	2.387 (2.452)	
	C−C	1.429 (1.429)	
	C−H	1.092 (1.092)	
	C_5, C−H	0.51 (−0.39)	
(η^5-C_5H_5)Ga	Ga−C	2.466 (2.489)	
	C−C	1.429 (1.429)	
	C−H	1.092 (1.092)	
	C_5, C−H	0.10 (−0.70)	
(η^5-C_5H_5)In	In−C	(2.641)	2.621(5)
	C−C	(1.430)	1.426(7)
	C−H	(1.092)	1.10(6)
	C_5, C−H	(−1.93)	−4.5(2)
(η^5-C_5Me_5)B	B−C	1.925 (2.041)	
	C−C	1.434 (1.436)	
	C−C(Me)	1.504 (1.504)	
	C_5, C−C	5.46 (3.31)	
(η^5-C_5Me_5)Al	Al−C	2.353 (2.422)	2.388(7)
	C−C	1.439 (1.440)	1.414(5)
	C−C(Me)	1.508 (1.508)	1.529(6)
	C_5, C−C	−2.41 (−3.74)	−5(2)
(η^5-C_5Me_5)Ga	Ga−C	2.439 (2.463)	2.405(4)
	C−C	1.440 (1.439)	1.420(3)
	C−C(Me)	1.507 (1.508)	1.522(3)
	C_5, C−C	−3.64 (−4.12)	−0.2(3)
(η^5-C_5Me_5)In	In−C	(2.622)	2.592(4)
	C−C	(1.440)	1.432(4)
	C−C(Me)	(1.509)	1.505(5)
	C_5, C−C	(−5.29)	−4.1(3)

[a] Bond distances in Å; bond angles in degrees. [b] Ring centroid−C−X (X = H, Me) defined as positive when substituents, X, point toward the metal and negative when they point away. [c] Results for basis set B in parentheses.

The nature of the π-type LUMOs and the highest occupied π-type orbitals are dependent upon the conjugative ability of the R substituent; representative examples of the LUMOs are shown in Figure 4. In the case of the MeM ligands, the p_x and p_y orbitals on the group 13 element are essentially vacant, while the (η^5-C_5R_5)M and $(H_3Si)_2NM$ ligands both feature donation from either the C_5R_5 π-orbitals or the nitrogen lone pair into the p_x and/or p_y orbitals on M. The significant difference between the π-donor substituents is that, whereas the η^5-C_5R_5 substitutent will donate electron density into both the p_x and p_y orbitals on M, the amido substituent can only donate into one. As the π-type orbitals on the group 13 element are formally vacant when R does not have the ability to donate π-electron density, the magnitude of π-donation can be quantified by the M $p_{x,y}$ orbital populations listed in Table 5. As expected, these interactions are the most important for boron and are illustrated in Figure 3. The most striking effect of this difference in π-overlap is found in the case of (η^5-C_5R_5)M, where the symmetry of the LUMO is different for M = B than for M = Al, Ga and In. For the boranediyl, the greater interaction between the π-type orbitals of the η^5-C_5R_5 ligand renders the antibonding e_1 pair π-acceptor orbital higher in energy than the e_2 orbital which

(33) Haaland, A.; Kjell-Gunnar, M.; Shlykov, S. A.; Volden, H. V.; Dohmeier, C.; Schnöckel, H. *Organometallics* **1995**, *14*, 3116.
(34) Haaland, A.; Kjell-Gunnar, M.; Volden, H. V.; Loos, D.; Schnöckel, H. *Acta Chem. Scand.* **1994**, *48*, 172.
(35) Beachley, O. T., Jr.; Blom, R.; Churchill, M. R.; Faegri, K., Jr.; Fettinger, J. C.; Pazik, J. C. Victoriano, L. *Organometallics* **1989**, *8*, 346.
(36) Starowieyski, K. B. In *Chemistry of Aluminium, Gallium, Indium and Thallium*; Downs, A. J., Ed.; Blackie Academic and Professional: London, 1993; Chapter 6 and references therein.
(37) This conclusion is based on Jemmis and Schleyer's orbital size explanation of cyclopentadienyl ring substituent deformation: Jemmis, E. D.; Schleyer, P. V. R. *J. Am. Chem. Soc.* **1982**, *104*, 4781.

Table 4. Calculated and Experimental Metrical Parameters for MeM and $(H_3Si)_2NM$ Ligands

	calculated[a]			experimental		
ligand	M−C	C−H	M−C−H	M−C (av)	compound	ref
MeB	1.5481 (1.5729)[b]	1.1102 (1.1092)	110.36 (110.27)	1.570 (4)	$(t\text{-BuB})_4$	38
MeAl	2.0104 (2.0408)	1.1109 (1.1102)	112.12 (112.33)	2.028 (5)	$[(Me_3Si)_3Al)]_4$	39
MeGa	2.0573 (2.0662)	1.1089 (1.1096)	111.47 (112.04)	2.08 (2)	$[(Me_3Si)_3CGa)]_4$	40
				2.064 (17)	$(Me_3Si)_3CGa$ (gas phase)	41
				2.100 (8)	$[(EtMe_2)_3CGa]_4$	42
MeIn	(2.2444)	(1.1089)	(112.23)	2.25 (1)	$[(Me_3Si)_3CIn)]_4$	22k, 43
				2.26 (1)	$[(EtMe_2)_3CIn]_4$	42

	M−N	N−Si	M−N−Si	Si−N−Si	M−N (av)	compound	ref
$(H_3Si)_2NB$	1.3880 (1.4070)	1.7970 (1.8020)	118.07 (117.98)	123.86 (124.04)	1.398 (7)	$(Me_2NB)_6$	44
$(H_3Si)_2NAl$	1.8620 (1.8960)	1.7560 (1.7570)	118.27 (119.06)	123.46 (121.89)	1.847 (2)	$(Me_3Si)_2NAl(Al(\eta^5\text{-}C_5Me_5))$	45
$(H_3Si)_2NGa$	1.9510 (1.9250)	1.7500 (1.7530)	117.06 (118.25)	125.88 (123.50)			
$(H_3Si)_2NIn$	(2.1180)	(1.7420)	(117.59)	(124.82)			

[a] Bond distances in Å; bond angles in degrees. [b] Results for basis set B in parentheses.

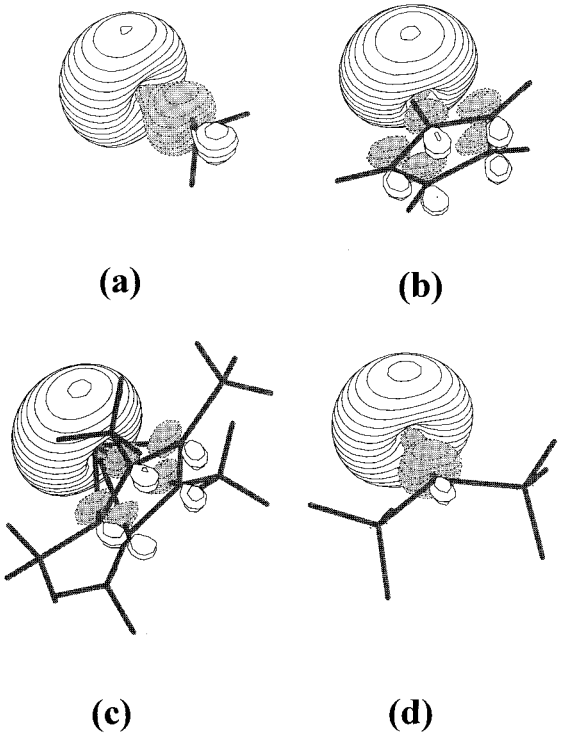

Figure 2. Three-dimensional representations of RB "lone pair" molecular orbitals: (a) MeB, (b) $(\eta^5\text{-}C_5H_5)B$, (c) $(\eta^5\text{-}C_5Me_5)B$, (d) $(H_3Si)_2NB$.

has no contribution from M and is localized on the $\eta^5\text{-}C_5R_5$ ring. For the heavier group 13 elements, the relatively weaker π-overlap leaves the e_1 pair as the LUMO (Figure 4).

In the case of the $(H_3Si)_2NB$ ligand, the nitrogen−boron bond order is close to 2 (1.92 on the basis of NBO analysis); hence, akin to amido-substituted carbenes and the isoelectronic vinylidene ligands, the predominant canonical form for this boranediyl is $(H_3Si)_2N{=}B{:}$. The heavier homologues have π-bonds that are more polarized toward the nitrogen atom than in the case of the boranediyl (Figure 5). The increased polarization of these π-interactions is presumably a consequence of the lower electronegativities of the other group 13 elements with respect to boron. Because the π-donation takes place exclusively to the p_y orbital of M, the LUMO in all cases possesses b_2 symmetry (dominated by the "nonbonding" p_x orbital[46] on M).

The relative amount of electron transfer between the substituent R and the group 13 element, M, can be estimated from

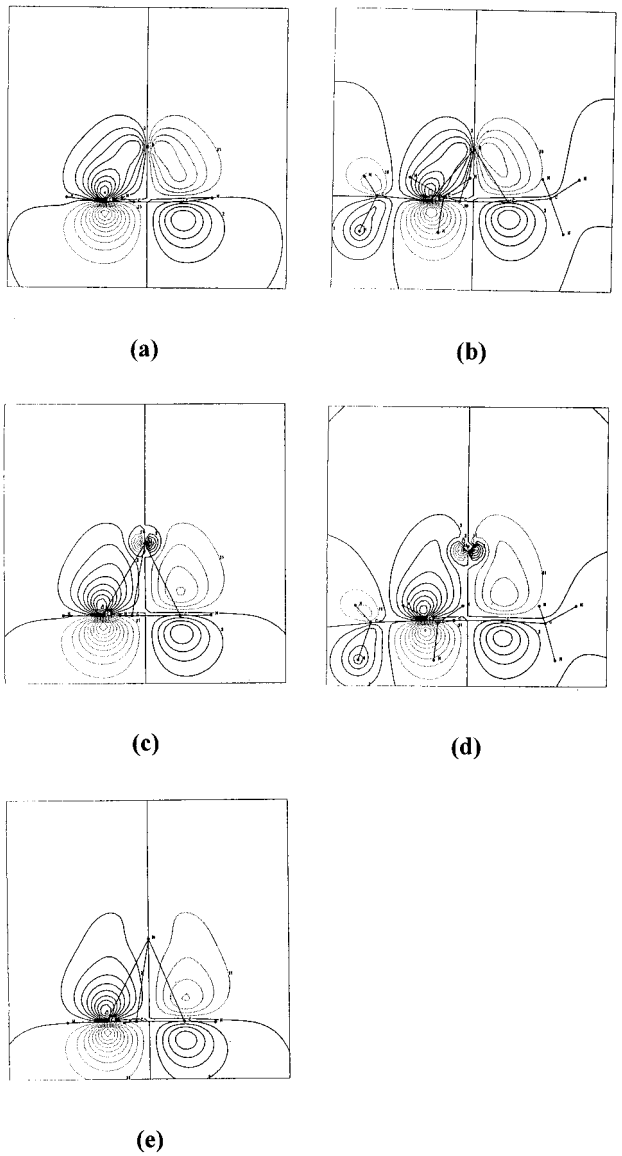

Figure 3. Contour diagram depictions of $(\eta^5\text{-}C_5R_5)M$ (R = H, Me) π-bonding molecular orbitals: (a) $(\eta^5\text{-}C_5H_5)B$, (b) $(\eta^5\text{-}C_5Me_5)B$, (c) $(\eta^5\text{-}C_5H_5)Al$, (d) $(\eta^5\text{-}C_5Me_5)Ga$, (e) $(\eta^5\text{-}C_5H_5)In$.

the charges on the M and R fragments for any given R. As shown in Table 6, for each R, the positive charge on boron is

(38) Mennekes, T.; Paetzold, P.; Boese, R.; Bläser, D. *Angew. Chem., Int. Ed. Engl.* **1991**, *30*, 173.

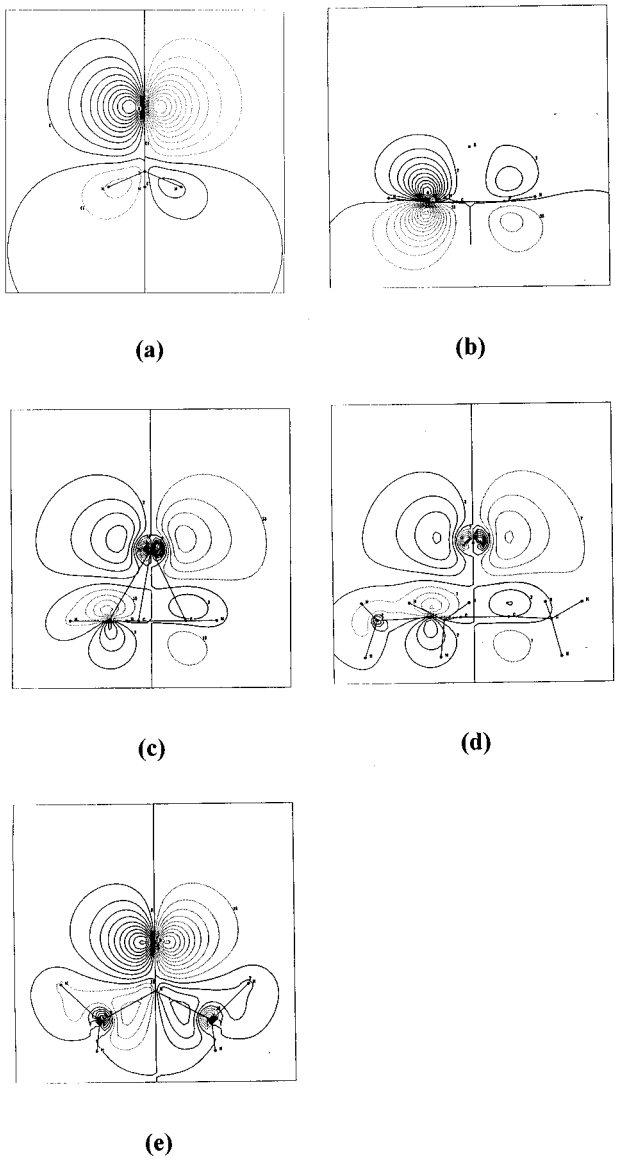

Figure 4. Contour diagram depictions of representative RM LUMOs: (a) MeB, (b) (η^5-C_5H_5)B, (c) (η^5-C_5H_5)Al, (d) (η^5-C_5Me_5)Ga, (e) $(H_3Si)_2$NB.

much lower than that on any other group 13 element. Again, this observation is anticipated on the basis of the trends in the electronegativities of the group 13 elements together with the more effective π-bonding capacity of boron. Comparison of the charge distributions associated with the different R groups suggests that the η^5-C_5R_5 ligands donate more electron density to (viewing R as an anion combining with an M^+ cation) or accept less electron density from (viewing R and M as radicals) the group 13 center than either the Me or $(H_3Si)_2N$ substituents. Also noteworthy is the somewhat surprising similarity of the charges on M for the ligands containing the methyl and amido groups despite the obvious difference in their conjugative abilities.

2. Iron Tetracarbonyl Complexes of RM Ligands. A useful starting point for the discussion of the iron tetracarbonyl complexes is to compare the computed $RMFe(CO)_4$ structures with the available experimental data. Because the series of iron tetracarbonyl complexes, (η^5-C_5Me_5)$MFe(CO)_4$ (M = B,[13] Al,[12] and Ga[9]), has been synthesized and structurally characterized, it is advantageous to commence with the cyclopentadienyl complexes. Note that the present calculations feature unsubstituted cyclopentadienyl ligands because (a) as shown earlier, the (η^5-C_5H_5)M and (η^5-C_5Me_5)M ligands are qualitatively very similar and (b) there is computational economy. The general level of agreement between the calculated and experimental structures is excellent, taking into account the weaker π-donating ability of the η^5-C_5H_5 vis-à-vis the η^5-C_5Me_5 ligand (Table 7). Like the experimentally observed pentamethylcyclopentadienyl-substituted boranediyl, alanediyl, and gallanediyl complexes referred to above, the model complexes (η^5-C_5H_5)$MFe(CO)_4$ (M = B, Al, Ga, In) feature a trigonal bipyramidal arrangement at the iron atom in which the (η^5-C_5H_5)M ligand adopts an axial site (Figure 6). Two anticipated trends are evident in the metrical parameters for the bonded (η^5-C_5H_5)M fragments. First, there is an increase in the computed M−Fe bond distance with an increase in the atomic number of M. Second, and as a consequence of employing the η^5-C_5H_5 rather than the η^5-C_5Me_5 ligand, the M−Fe and M−C bond distances are longer than those measured experimentally with the exception of (η^5-C_5H_5)B. A further conspicuous trend is the appreciable shortening of the M−C bond distances of the (η^5-C_5H_5)M ligands upon complexation. Such shortening is expected on the basis of the increased charge on M which contracts the orbitals involved in Cp-M bonding and because complexation effectively depopulates the partially Cp-M antibonding "lone pair" orbital. This type of R−M contraction upon depopulation of the "lone pair" orbital of M has also been observed previously in quantum chemical investigations of R−M oligomerization reactions,[22] although there is rehybridization of the "lone pair" orbital in such cases.

As in the case of the free ligands, an interesting structural facet of the model (η^5-C_5H_5)$MFe(CO)_4$ complexes is the bending of the cyclopentadienyl hydrogen atoms out of the C_5 plane. For each M, the extent of deformation toward M is found to increase significantly upon complexation: the differences in the angles of deformation between uncomplexed and complexed ligands vary from 0.6° for (η^5-C_5H_5)In to more than 3° for (η^5-C_5H_5)B. Such a trend is only consistent with a covalent bonding model for the CpM ligands despite the increased Cp^-M^+ charge separation (vide infra) and is in agreement with Jemmis and Schleyer's orbital size explanation of cyclopentadienyl ring substituent deformation.[37]

To the best of our knowledge, no base-free complexes have been isolated in which an (alkyl)M ligand coordinates to iron in a terminal fashion. Accordingly, this type of complex has been examined by DFT methods. Important structural parameters for the $MeMFe(CO)_4$ model complexes are listed in Table 7 and a drawing of a typical structure is presented in Figure 6. Like their (η^5-C_5H_5)M analogues, the $MeMFe(CO)_4$ complexes possess trigonal bipyramidal geometries, and the group 13 ligands occupy one of the axial sites. Interestingly, the $Fe(CO)_4$

(39) Schnitter, C.; Roesky, H. W.; Röpken, C.; Herbst-Irmer, R.; Schmidt, H.-G.; Noltemeyer, M. *Angew. Chem., Int. Ed.* **1998**, *37*, 1952.
(40) Uhl, W.; Hiller, W.; Layh, M.; Schwarz, W. *Angew. Chem., Int. Ed. Engl.* **1992**, *31*, 1364.
(41) Haaland, A.; Martinsen, K.-G.; Volden, H. V.; Kaim, W.; Waldhör, E.; Uhl, W.; Schütz, U. *Organometallics* **1996**, *15*, 1146.
(42) Uhl, W.; Jantschak, A. *J. Organomet. Chem.* **1998**, *555*, 263.
(43) (a) Schluter, R. D.; Cowley, A. H.; Atwood, D. A.; Jones, R. A.; Atwood, J. L. *Coord. Chem.* **1993**, *30*, 35. (b) Uhl, W.; Graupner, R.; Layh, M.; Schütz, U. *J. Organomet. Chem.* **1995**, *493*, C1.
(44) Nöth, H.; Pommerening, H. *Angew. Chem., Int. Ed. Engl.* **1980**, *19*, 482.
(45) Sitzmann, H.; Lappert, M. F.; Dohmeier, C.; Üffing, C.; Schnöckel, H. *Organomet. Chem.* **1998**, *561*, 203.
(46) The standard assignment for the p_x and p_y orbitals on the $(H_3Si)_2$NM ligands has been reversed to conform to that of the $(H_3Si)_2$NB$Fe(CO)_4$ complex discussed below.

Table 5. Dipole Moments and NBO π-Orbital Populations (Electrons) for RM Ligands

compound	dipole moment	M $p_{x,y}$ orbital population
MeB	−2.9771 (−3.1287)[a]	0.03775 (0.03392)
MeAl	−0.9719 (−0.8545)	0.01 (0.00978)
MeGa	−0.7967 (−0.5636)	0.00937 (0.00932)
MeIn	(−0.1594)	(0.00697)
(η^5-C_5H_5)B	−2.9414 (−2.61)	0.30364 (0.25643)
(η^5-C_5H_5)Al	−1.2913 (−0.7932)	0.15196 (0.14859)
(η^5-C_5H_5)Ga	−0.3995 (−0.1963)	0.16732 (0.15768)
(η^5-C_5H_5)In	(0.3443)	(0.14686)
(η^5-C_5Me_5)B	−3.4927 (−3.2058)	0.31502 (0.24823)
(η^5-C_5Me_5)Al	−2.0561 (−1.6247)	0.14184 (0.1403)
(η^5-C_5Me_5)Ga	−1.2676 (−1.0327)	0.16167 (0.15076)
(η^5-C_5Me_5)In	(−0.4595)	(0.1411)

	dipole moment	M p_y	M p_x
$(H_3Si)_2NB$	−3.5349 (−3.5892)	0.21774 (0.21491)	0.06379 (0.05918)
$(H_3Si)_2NAl$	−0.0914 (0.1968)	0.10757 (0.11277)	0.0182 (0.01694)
$(H_3Si)_2NGa$	0.5369 (0.5724)	0.11445 (0.11378)	0.01877 (0.01729)
$(H_3Si)_2NIn$	(1.66)	(0.09786)	(0.01412)

[a] Results for basis set B in parentheses.

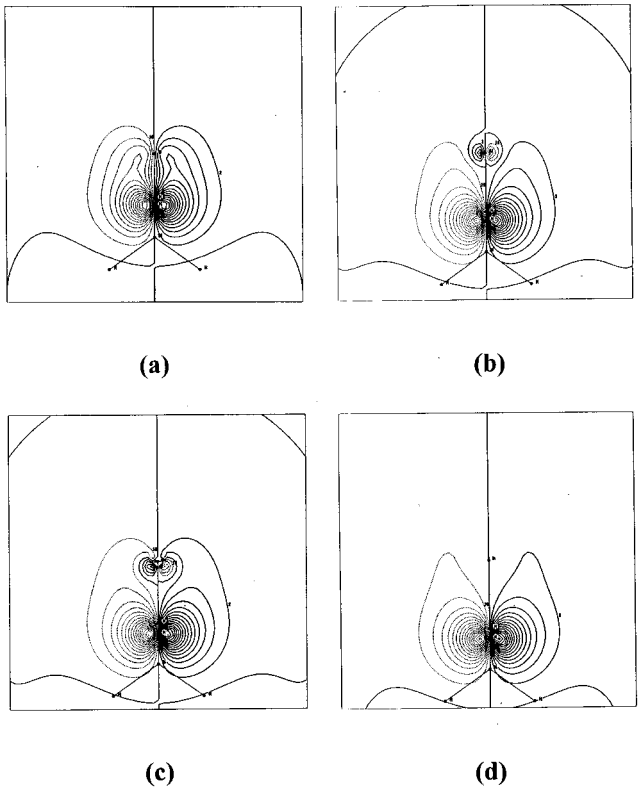

Figure 5. Contour diagram depictions of $(H_3Si)_2NM$ N−M π-bonding molecular orbitals: (a) M = B, (b) M = Al, (c) M = Ga, (d) M = In.

moiety is much less distorted in the MeM complexes. A further difference between the (η^5-C_5H_5)M and MeM complexes is that there is significantly less contraction of the M−C bonds upon coordination in the case of the latter. However, the most striking structural feature of this series of complexes is the extremely short B−Fe bond distance, [1.794 (1.806) Å] which is approximately 9% shorter than that of the corresponding (η^5-C_5H_5)B complex. In sharp contrast, the group 13 element−iron bond distances for the heavier congeneric RMFe(CO)$_4$ complexes are nearly identical (<3% difference) for R = Me and η^5-C_5H_5. In turn, the short B−Fe bond distance suggests that the alkyl-substituted boranediyl complexes may represent the best prospect for a modicum of iron−group 13 element back-bonding. In support of such a postulate, it is worth noting that

Table 6. Selected NBO Charge Distributions (au) for RM Ligands

compound	q (M)	q (R)
MeB	0.46475 (0.47534)[a]	−0.46475 (−0.47534)
MeAl	0.72358 (0.73687)	−0.72358 (−0.73687)
MeGa	0.68179 (0.70915)	−0.68179 (−0.70915)
MeIn	(0.70646)	(−0.70646)
(η^5-C_5H_5)B	0.09853 (0.28921)	−0.09853 (−0.28921)
(η^5-C_5H_5)Al	0.58461 (0.62054)	−0.58461 (−0.62054)
(η^5-C_5H_5)Ga	0.57012 (0.60435)	−0.57012 (−0.60435)
(η^5-C_5H_5)In	(0.64139)	(−0.64139)
(η^5-C_5Me_5)B	0.07726 (0.30139)	−0.07726 (−0.30139)
(η^5-C_5Me_5)Al	0.61591 (0.64262)	−0.61591 (−0.64262)
(η^5-C_5Me_5)Ga	0.58444 (0.62077)	−0.58444 (−0.62077)
(η^5-C_5Me_5)In	(0.65599)	(−0.65599)
$(H_3Si)_2NB$	0.47873 (0.49686)	−0.47873 (−0.49686)
$(H_3Si)_2NAl$	0.79175 (0.79534)	−0.79175 (−0.79534)
$(H_3Si)_2NGa$	0.75587 (0.77544)	−0.75587 (−0.77544)
$(H_3Si)_2NIn$	(0.79683)	(−0.79683)

[a] Results for basis set B in parentheses.

MeBFe(CO)$_4$ complex is the only one that exhibits significant differences in the metrical parameters of the Fe(CO)$_4$ moiety. Specifically, the axial C−Fe bond distance is longer than that found in any of the other model complexes, and the trans-C−O bond distance is also slightly shorter than the typical length. Such structural changes are consistent with reduced OC ← Fe back-bonding—the anticipated consequence of a B ← Fe back-bonding interaction.

Since the RMFe(CO)$_4$ complexes can be viewed as being formed by the combination of singlet RM and Fe(CO)$_4$ fragments, insights into the nature of the M−Fe bonding description can be gleaned from an examination of the pertinent frontier orbitals of these moieties. The primary interaction is anticipated to be that between the "lone pair" donor orbital (usually the HOMO) on RM and the acceptor LUMO on Fe(CO)$_4$. The frontier orbital energies of the alane-, gallane-, and indanediyls are quite similar to one another for a given R substituent. However, for (η^5-C_5H_5)B the energy of the donor HOMO is higher than those for the heavier congeners, thus suggesting that this ligand will be the strongest σ-donor. In contrast, the HOMO of MeB is somewhat lower in energy than those of its heavier congeners and is even lower in energy than the HOMO of (η^5-C_5H_5)B. Conversely, the HOMO energies of the heavier MeM ligands are all higher than those of the

Table 7. Selected Structural Parameters for $RMFe(CO)_4$ Complexes

$(\eta^5\text{-}C_5H_5)MFe(CO)_4$ Complexes

M	M−C (av)[a]	M−X[b]	C−C (av)	C−H (av)	M−C−H (av)	X−C−H (av)
B	1.835 (1.863)[c] [1.814][d]	1.374 (1.411) [1.347]	1.430 (1.431) [1.428]	1.090 (1.090)	122.687 (122.024)	10.870 (10.776)
Al	2.241 (2.289) [2.147]	1.879 (1.936)	1.435 (1.435)	1.091 (1.091)	121.725 (121.542)	1.549 (0.787)
Ga	2.318 (2.321) [2.226]	1.970 (1.974)	1.436 (1.435)	1.091 (1.091)	121.033 (121.154)	0.871 (−0.645)
In	(2.497)	(2.179)	(1.435)	(1.092)	(120.365)	(−1.301)

M	M−Fe	X−M−Fe	Fe−C(ax)	C−O(ax)	Fe−C(eq) (av)	C−O(eq) (av)
B	1.972 (1.954) [2.010(3)]	180.000 (180.000) [178.6]	1.795 (1.795) [1.793(3)]	1.169 (1.168) [1.148(4)]	1.772 (1.774) [1.778]	1.179 (1.178) [1.151]
Al	2.243 (2.277) [2.231(3)]	180.000 (180.000) [176]	1.777 (1.774) [1.796(10)]	1.169 (1.169)	1.780 (1.782) [1.766]	1.177 (1.176)
Ga	2.289 (2.298) [2.2731(4)]	179.294 (179.294)	1.767 (1.768) [1.781(2)]	1.169 (1.169) [1.143(3)]	1.788 (1.787) [1.789]	1.174 (1.174) [1.145]
In	(2.445)	(179.163)	(1.762)	(1.169)	(1.790)	(1.174)

$MeMFe(CO)_4$ Complexes

M	M−C	C−H (av)	M−C−H (av)
B	1.536 (1.536)	1.107 (1.106)	110.87 (110.69)
Al	1.966 (1.986)	1.105 (1.105)	110.75 (110.93)
Ga	1.982 (1.982)	1.104 (1.104)	109.79 (110.37)
In	(2.154)	(1.103)	(110.10)

M	M−Fe	C−M−Fe	Fe−C(ax)	C−O(ax)	Fe−C(eq) (av)	C−O(eq) (av)
B	1.794 (1.806)	180.00 (180.00)	1.838 (1.836)	1.163 (1.163)	1.783 (1.784)	1.171 (1.170)
Al	2.203 (2.238)	180.00 (180.00)	1.787 (1.785)	1.167 (1.167)	1.782 (1.783)	1.175 (1.175)
Ga	2.218 (2.237)	180.00 (180.00)	1.785 (1.784)	1.167 (1.167)	1.786 (1.786)	1.174 (1.174)
In	(2.386)	(180.00)	(1.776)	(1.168)	(1.787)	(1.175)

$(H_3Si)_2NBFe(CO)_4$

B−N	N−Si	B−N−Si	Si−N−Si
1.377	1.800	119.36	121.27

B−Fe	N−B−Fe	Fe−C(ax)	C−O(ax)	Fe−C(eq) (av)	C−O(eq) (av)
1.835	178.62	1.818	1.165	1.781	1.172

[a] Bond distances in Å; bond angles in degrees. [b] X = η^5-C_5H_5 ring centroid. [c] Results for basis set B in parentheses. [d] Experimental data for $(\eta^5\text{-}C_5H_5)MFe(CO)_4$ complexes in square brackets.

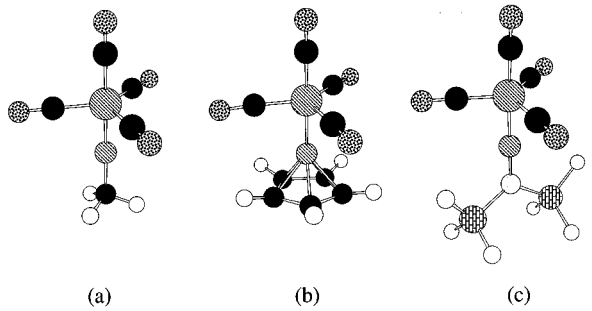

(a) (b) (c)

Figure 6. Drawings of representative complexes: (a) $MeMFe(CO)_4$, (b) $(\eta^5\text{-}C_5H_5)MFe(CO)_4$ and (c) $(H_3Si)_2NBFe(CO)_4$.

cyclopentadienyl analogues. Because of the superior π-acceptor ability of boron (vide supra) the LUMO of $(\eta^5\text{-}C_5H_5)B$ is higher in energy (and of different symmetry) than those of the heavier $(\eta^5\text{-}C_5H_5)M$ ligands (M = Al, Ga, In), and will thus be a less suitable acceptor for back-bonding. Moreover, the LUMO of MeB is also lower in energy than are those of the heavier analogues, and in fact, it possesses the lowest energy LUMO of all the RM ligands. It is concluded that MeB would be the best back-bond acceptor in the series of compounds considered here.

Some important changes take place in the aforementioned frontier orbitals upon coordination of the RM ligands. As stated above, the primary geometrical change is shortening of the M−C bonds. In the cases of $(\eta^5\text{-}C_5H_5)Ga$ and $(\eta^5\text{-}C_5H_5)In$, the most significant change that accompanies coordination to the $Fe(CO)_4$ fragment is that the HOMO becomes a "lone pair" orbital of symmetry a rather than a π-bond of symmetry e. This change in orbital sequence allows these ligands to interact with the $Fe(CO)_4$ orbitals in a fashion similar to that of their lighter homologues. A similar destabilization of the "lone pair" orbital and other valence orbitals, along with minor stabilization of the LUMOs, is also observed for the other $(\eta^5\text{-}C_5H_5)M$ ligands. That the totally symmetric orbital is destabilized more extensively than the e orbitals is presumably a consequence of the symmetry and the partially Cp−M antibonding nature of the former. Obviously, reduction of the cyclopentadienyl−metal distance will affect this orbital more than the π-bonding e-type orbitals. In the case of the MeM ligands, however, there is no change in orbital sequence and virtually no change in orbital energy, as expected on the basis of the virtually insignificant structural changes that take place upon complexation to the $Fe(CO)_4$ fragment.

The charge distributions for the RM and $Fe(CO)_4$ fragments change significantly upon formation of the $RMFe(CO)_4$ complexes as summarized in Table 9. Note that the RM ligand is a net electron donor to the iron tetracarbonyl fragment in each case. The negative charge on the iron atom is significantly larger

Table 8. Selected Properties of RM Ligands and Fe(CO)$_4$ in Coordinated Geometries[a]

	dipole moment	M $p_{x,y}$ population	q (M)	q (R)	q (Fe)
MeB	−3.0422 (−3.2957)[b]	0.0386 (0.0370)	0.4639 (0.4698)	−0.4639 (−0.4698)	−0.0600 (−0.0601)
MeAl	−1.1155 (−1.0397)	0.0108 (0.0107)	0.7281 (0.7411)	−0.7281 (−0.7411)	−0.0797 (−0.0789)
MeGa	−1.1073 (−0.8852)	0.0109 (0.0108)	0.6852 (0.7134)	−0.6852 (−0.7134)	−0.0789 (−0.0786)
MeIn	(−0.5180)	(0.0079)	(0.7106)	(−0.7106)	(−0.0727)
(η^5-C_5H_5)B	−3.6386 (−3.7862)	0.3313 (0.2816)	−0.0155 (0.1530)	0.0155 (−0.1530)	−0.0819 (−0.0823)
(η^5-C_5H_5)Al	−2.3195 (−1.8542)	0.1663 (0.1540)	0.5714 (0.6190)	−0.5714 (−0.6190)	−0.0861 (−0.0851)
(η^5-C_5H_5)Ga	−1.4085 (−1.2729)	0.1635 (0.1501)	0.5588 (0.6016)	−0.5588 (−0.6016)	−0.0864 (−0.0850)
(η^5-C_5H_5)In	(−0.6195)	(0.1423)	(0.6380)	(−0.6380)	(−0.0846)
$(H_3Si)_2$NB	5.5774	p_x 0.2188 p_y 0.0643	0.4770	−0.4770	−0.06980

[a] All properties reported in atomic units. [b] Results for basis set B in parentheses.

Table 9. Group 13 Element π-Orbital Populations and NBO Charges for RMFe(CO)$_4$ Complexes[a]

	M $p_{x,y}$ population	q(M)	q(R)	q(Fe)	q(Fe(CO)$_4$)	q(MR)
			MeMFe(CO)$_4$			
B	0.34772 (0.35271)[b]	0.64327 (0.70213)	−0.30035 (−0.35084)	−0.56219 (−0.56714)	−0.34292 (−0.35129)	0.34292 (0.35129)
Al	0.18695 (0.18178)	1.28430 (1.32313)	−0.53387 (−0.55879)	−0.61213 (−0.60591)	−0.75043 (−0.76434)	0.75043 (0.76434)
Ga	0.18243 (0.17813)	1.13439 (1.21359)	−0.46656 (−0.51743)	−0.69562 (−0.59647)	−0.66783 (−0.69616)	0.66783 (0.69616)
In	(0.13278)	(1.44050)	(−0.21440)	(−2.27909)	(−1.22610)	(1.22610)
			CpMFe(CO)$_4$			
B	0.50032 (0.48227)	0.29071 (0.54982)	0.18517 (0.17585)	−0.48884 (−1.81023)	−0.47587 (1.08456)	0.47587 (−1.08456)
Al	0.28753 (0.27373)	1.14915 (1.19955)	−0.47907 (−0.53196)	−0.58138 (−0.57533)	−0.67008 (−0.66759)	0.67008 (0.66759)
Ga	0.28160 (0.27086)	0.95017 (1.04414)	−0.45070 (−0.50391)	−0.53406 (−0.49771)	−0.49948 (−0.54023)	0.49948 (0.54023)
In	(0.23427)	(1.15836)	(−0.45098)	(−0.52940)	(−0.70738)	(0.70738)

[a] All data in atomic units. [b] Results for basis set B in parentheses.

than that on Fe(CO)$_4$ or Fe(CO)$_5$ (more than 0.5 except when M = B). Upon complexation, the positive charge on M increases, and the negative charge on the R substituent of each ligand decreases, but to a lesser extent. Within each homologous series the largest positive charge on M is found for Al, followed by In, Ga, and B as expected on the basis of electronegativity considerations. For M = Al, Ga, and In there are similar overall charges on the RM fragments with slightly larger charges being found for the methylated species. Once again, the boranediyl complexes exhibit markedly different behavior. The positive charge on the (η^5-C_5H_5)B ligand (0.474) is larger than that on MeB (0.343) despite the larger positive charge on the boron atom in the latter [(η^5-C_5H_5)B: 0.291; MeB: 0.643]. Each boranediyl ligand has a smaller positive charge than those of any of the other RM ligands. Consequently the negative charge on the Fe(CO)$_4$ fragment of each boranediyl complex is smaller than those found on the heavier analogues. The difference between the borane- and alanediyl complexes is most pronounced for the methyl derivatives, where the positive charge on MeAl is over 0.4 greater than that on MeB (compared to a difference of only 0.194 between (η^5-C_5H_5)B and (η^5-C_5H_5)-Al).

Analysis of the group 13 element $p_{x,y}$-orbital electron populations in the MeMFe(CO)$_4$ complexes provides a measure of the M ← Fe π-back-bonding. These orbitals are essentially vacant in the uncoordinated ligands (in both the free and coordinated geometries), and barring hyperconjugation from the methyl group C−H bonds, the only source of π-electron density must be the Fe(CO)$_4$ fragment. Two features are readily apparent in the data presented in Table 8: (1) the π-orbital populations on each of the MeM ligands are increased upon coordination, and more significantly, (2) the π-electron population on the boron atom [0.348 (0.353) electron per orbital] is almost twice as large as that on any of the heavier elements [e.g., 0.187 (0.182) electron per orbital for Al]. The total π-electron population on boron is thus 0.696 electron in MeBFe(CO)$_4$ and clearly displays the maximum amount of back-bonding in any of the RMFe(CO)$_4$ complexes considered here.

It is noteworthy that the π-orbital populations on M in the cyclopentadienyl complexes, (η^5-C_5H_5)MFe(CO)$_4$ (Table 9) are all larger than those for the corresponding methyl complexes, MeMFe(CO)$_4$. This is a consequence of the π-donating ability of the (η^5-C_5H_5) group. As discussed earlier, the p_x and p_y orbitals on the (η^5-C_5H_5)M ligands are already appreciably populated prior to coordination, and these populations are not significantly different in the coordinated geometry. It is therefore tempting to postulate that the increased π-electron populations on the group 13 elements in the (η^5-C_5H_5)MFe(CO)$_4$ complexes are due to Fe → M π-back-bonding. However, examination of the bonding molecular orbitals (vide infra) demonstrates clearly that this is not the case, leading to the conclusion that the increased π-electron population is a consequence of increased (η^5-C_5H_5) to M π-bonding. The single-point calculations for the (η^5-C_5H_5)M ligands in their coordinated geometries do not account for the loss of total electron density from the ligands and the concomitant increases in the charges on M found in the (η^5-C_5H_5)MFe(CO)$_4$ complexes. That the increased effective nuclear charge of M will result in more extensive cyclopentadienyl−metal bonding is consistent with the observed shortening of the cyclopentadienyl−group 13 element distance upon complexation. Confirmation of the view that the increased π-electron population results almost exclusively from the increased charge on boron is provided by an analysis of the protonated boranediyl, [(η^5-C_5H_5)BH]$^+$. The NBO valence p_x and p_y populations on boron for this cation are 0.503 e for both basis sets A and B, which is almost exactly the same as those found for (η^5-C_5H_5)BFe(CO)$_4$, leading to the conclusion that the (η^5-C_5H_5)M ligands are not efficient π-acceptors even in the case of M = B.

The foregoing conclusions regarding the π-acceptor characteristics of the RM ligands that were deduced on the basis of frontier orbital properties and other criteria discussed previously

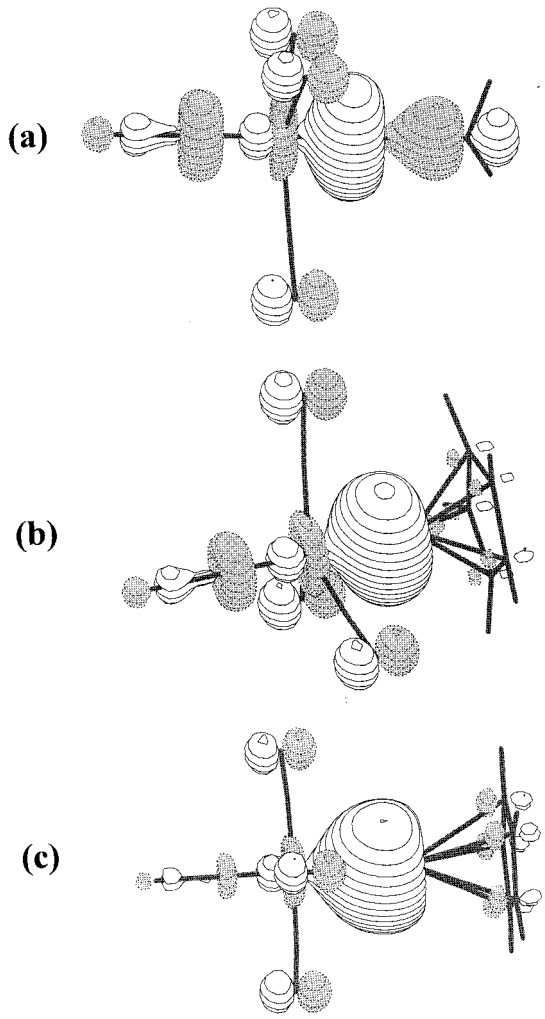

Figure 7. Three-dimensional depictions of representative RM → Fe(CO)$_4$ σ-bond molecular orbitals: (a) RM = MeB, (b) RM = (η^5-C$_5$H$_5$)B, (c) RM = (η^5-C$_5$H$_5$)In.

are confirmed by analysis of the pertinent molecular orbitals of the RMFe(CO)$_4$ complexes. The first point of interest is that, for a given substituent, there is a striking similarity in the orbitals despite the expected stronger interaction between the HOMO on the RB ligands and the LUMO on the Fe(CO)$_4$ fragment. The orbitals for the (η^5-C$_5$H$_5$)MFe(CO)$_4$ complexes are similar to each other when M = B and Al and slightly different for M = Ga and In (there is an extra pair of essentially degenerate orbitals higher in energy than the M−Fe bonding orbitals). The situation is similar for the MeMFe(CO)$_4$ complexes; however, the energy of the B−Fe bonding orbital is significantly lower than those of any of the heavier congeners and also lower than that of the (η^5-C$_5$H$_5$)B complex.

Contour diagrams and three-dimensional pictures of the important molecular orbitals provide convincing evidence of the nature of the bonding in the RMFe(CO)$_4$ complexes (Figure 7). The a′ orbital primarily attributable to "lone pair" coordination of M to the Fe center is remarkably similar in each RMFe(CO)$_4$ complex. Examples of these MOs clearly illustrate that, regardless of the nature of R or M, the M−Fe interaction take place primarily between the "lone pair" orbital on RM and the d_{z^2} orbital on iron and results in an onion-shaped bonding combination. The π-type orbitals are of particular interest with respect to the question of M ← Fe back-bonding. The π-bonding, nonbonding or potentially π-accepting interactions for the (η^5-C$_5$H$_5$)MFe(CO)$_4$ complexes are shown in Figure 8. These

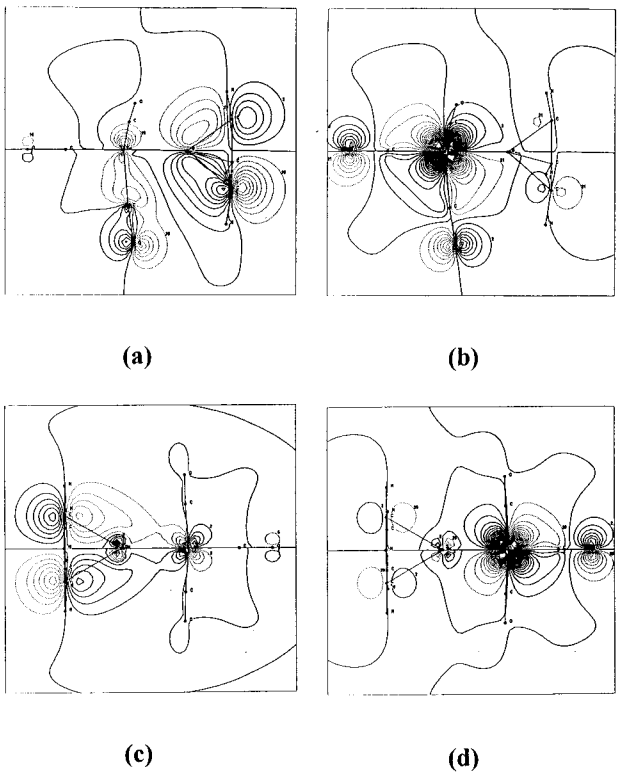

Figure 8. Contour diagrams of representative π-type molecular orbitals for (η^5-C$_5$H$_5$)MFe(CO)$_4$ complexes: (a) M = B HOMO−3, (b) M = B HOMO−1, (c) M = Ga HOMO−2, (d) M = Ga HOMO−1.

orbitals are qualitatively similar for each complex; however, the energetic ordering is dependent upon the group 13 element. In each (η^5-C$_5$H$_5$)MFe(CO)$_4$ complex the p_x and p_y orbitals on M interact almost exclusively with the cyclopentadienyl ligand. For the boranediyl complex, the orbital pair (a′ and a″) corresponding to (η^5-C$_5$H$_5$)−boron π-bonding is the HOMO−3 orbital [energy: −0.31797 (−0.31505) au] which is located directly below the B → Fe σ-bonding MO [energy: −0.26771 (−0.26995) au]. The particularly strong B → Fe σ-interaction results in a relatively high-energy B−Fe σ-antibonding orbital [LUMO+1 (a′); energy: −0.03673 (−0.03557) au] directly below the doubly degenerate π-antibonding orbitals [LUMO+2 (a′ and a″); energy: −0.03046 (−0.03084) au]. The HOMO [(a′ and a″) energy: −0.17959 (−0.17915) au] and LUMO [(a′ and a″) energy: −0.06572 (−0.06302) au] are located primarily on the Fe(CO)$_4$ fragment. The only obvious indication of π-back-bonding is found in the HOMO−1 orbital [(a′ and a″) energy: −0.22025 (−0.21982) au] which involves an interaction between Fe and the CO ligand trans to the boranediyl ligand.

The ordering of bonding orbitals for (η^5-C$_5$H$_5$)AlFe(CO)$_4$ is similar to that for the boranediyl complex in that the doubly degenerate (η^5-C$_5$H$_5$)-Al π-bond pair [(a′ and a″) energy: −0.28311 (−0.27965) au] appears below the Al−Fe σ-bond orbital [(a′) energy: −0.25726 (−0.26042) au]. However, the relatively weaker Al → Fe σ-interaction causes the σ-antibonding orbital to become the LUMO in the alanediyl complex [(a′) energy: −0.07943 (−0.08468) au]. The Al−Fe π-antibonding interaction is once again represented by the LUMO+2 orbital [(a′ and a″) energy: −0.04941 (−0.04699) au] and there is no indication of Al←Fe back-bonding.

The sequence of antibonding orbitals for the (η^5-C$_5$H$_5$)Ga and (η^5-C$_5$H$_5$)In complexes is similar to that found for the alanediyl analogue. As indicated earlier, the only significant change in the ordering of the bonding orbitals is the reversal of

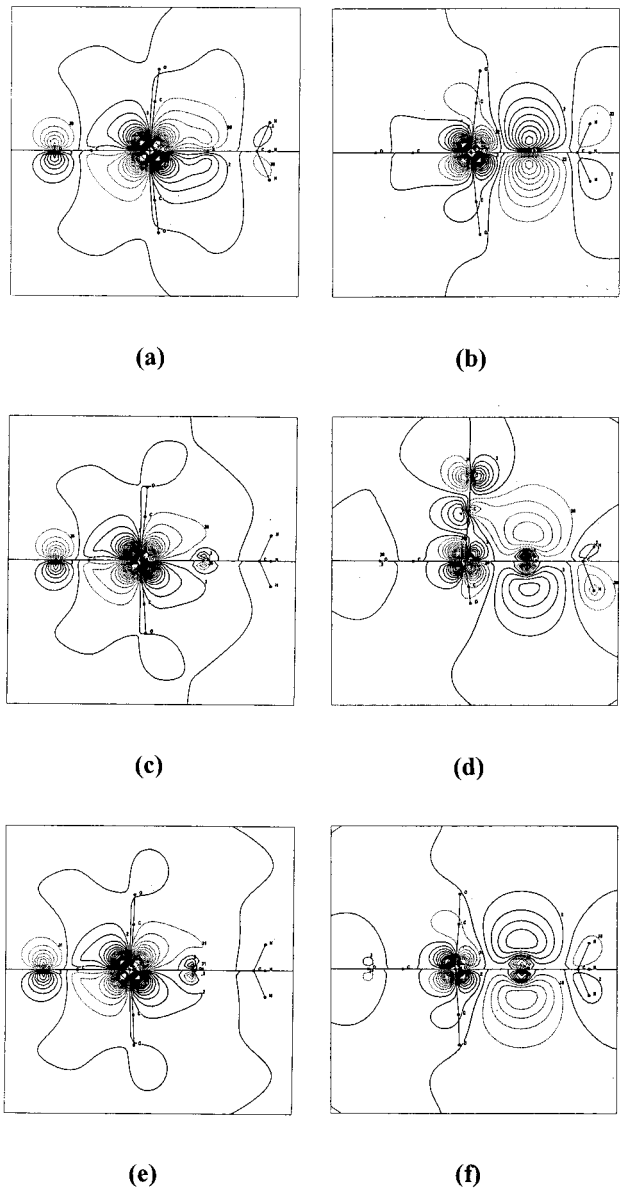

Figure 9. Contour diagrams of representative π-type molecular orbitals for MeMFe(CO)$_4$ complexes: (a) M = B HOMO−1, (b) M = B LUMO, (c) M = Al HOMO−1, (d) M = Al LUMO, (e) M = Ga HOMO−1, (f) M = Ga LUMO.

M−Fe σ bond and (η^5-C_5H_5)-M π-bond energy levels (as found in the uncoordinated (η^5-C_5H_5)M ligands). A possible reason for the reversed ordering is that the relatively weaker π-acceptor properties of gallium and indium complexes result in less stable π-bonding interactions.

The bonding descriptions for the MeMFe(CO)$_4$ complexes are considerably different from those for the cyclopentadienyl analogues due to the loss of R−M π-bonding. A selection of important bonding, antibonding and potentially π-accepting orbitals is presented in Figure 9. As in the case of the (η^5-C_5H_5)-MFe(CO)$_4$ complexes, the a′ orbital responsible for M → Fe σ-bonding is formed primarily by interaction of the "lone pair" on M and the iron d_{z^2} orbital. The ordering of each of the occupied orbitals in the MeMFe(CO)$_4$ complexes is independent of the group 13 element. The HOMO is an essentially Fe(CO)$_4$-based orbital pair (a′ and a″), and the σ-bonding interaction is the HOMO−2 orbital for each complex. Of note, however, is the relatively low energy of this orbital when M = B [energy: −0.29968 (−0.29911) au] compared with the heavier analogues [M = Al, energy: −0.25740 (−0.25620) au; M = Ga, energy: −0.26093 (−0.25948) au]. In turn, this suggests a stronger interaction in the case of the boranediyl complex. The HOMO−1 orbital pair (a′ and a″) of MeBFe(CO)$_4$ is of particular interest because these feature significant M ← Fe π-back-bonding (Figure 10). In the case of MeBFe(CO)$_4$ the HOMO−1 orbital [energy: −0.26673 (−0.26506) au] exhibits a bonding overlap of the empty boron p_x (p_y) orbital with the iron d_{xz} (d_{yz}) orbital, which overlaps in a similar fashion with a carbon p orbital of the axial CO ligand. Although the doubly degenerate HOMO−1 orbital pairs for the heavier analogues are similar in overall appearance to that of the boranediyl complex, the extent of M ← Fe back-bonding is reduced considerably. The magnitude of the wave function for the M ← Fe back-bond when M = B is much larger and more obviously directed toward M than for the corresponding alane- or gallanediyl complexes. Consequently, the magnitude of the wave function corresponding to the axial OC ← Fe back-bond increases as M is changed from boron to the heavier elements, which is in accord with the structural features noted previously. The LUMO of each MeMFe(CO)$_4$ complex is a doubly degenerate M−Fe π-antibonding orbital pair (a′ and a″), and the M−Fe σ-antibonding orbital (a′) is the LUMO+1 (Figure 9).

The M−Fe bond energies for the RMFe(CO)$_4$ complexes (Table 10) reveal several distinct trends that complement the conclusions that were reached on the basis of structural data and orbital analyses. For a given substituent, R, the bond energy decreases as the atomic number of M increases, thus the boranediyl ligands form the most stable iron tetracarbonyl complexes. As expected, the MeM ligands form stronger M−Fe bonds than do the analogous (η^5-C_5H_5)M ligands. The most noteworthy feature of the bond energies is that the B−Fe energy for MeBFe(CO)$_4$ [108.87 (111.36) kcal/mol] is significantly larger than that for (η^5-C_5H_5)BFe(CO)$_4$ [89.24 kcal/mol]. All of the RM ligands except (η^5-C_5H_5)Ga and (η^5-C_5H_5)In have M−Fe bonds that are stronger than the C−Fe bond [56.46 kcal/mol][47] of an axial carbonyl substituent in Fe(CO)$_5$ and are thus quite effective ligands. The greater strength of the M−Fe bond also suggests that many RMFe(CO)$_4$ complexes should be synthetically accessible by reaction of the RM(I) ligand with iron pentacarbonyl (vide infra).

As expected, the energies of reaction of the RM ligands with the Fe(CO)$_4$ fragment show the same trends as the M−Fe bond energies. The relevant bond energies are listed in Table 10 from which it is evident that all of the reactions are appreciably exothermic. A derivation of Zeigler's reaction energy analysis[28] provides further information concerning the activation energies of complexation. In this approach, the donor and acceptor components of the complex are forced into their coordinated geometries. This provides insight into the amount of energy required to reorganize the ground-state structures in addition to the changes in electronic structures of the reactants. Furthermore, this type of analysis provides insights into the origin of exothermicity (in this case) of the reaction

$$\mathrm{RM} + \mathrm{Fe(CO)_4} \rightarrow \mathrm{RMFe(CO)_4} \quad (1)$$

$$E_{\mathrm{rxn}} = E_{\mathrm{prep}} + E^\circ + E_{\mathrm{int}} \quad (2)$$

The energy of reaction, E_{rxn}, is deconstructed into three components (eq 2), namely the reorganization energies of the "reactants", E_{prep}, the energy of electrostatic attraction and Pauli repulsion between the "reactants" (steric energy), E°, and the

(47) This energy is higher than that obtained with different DFT methods; see ref 21.

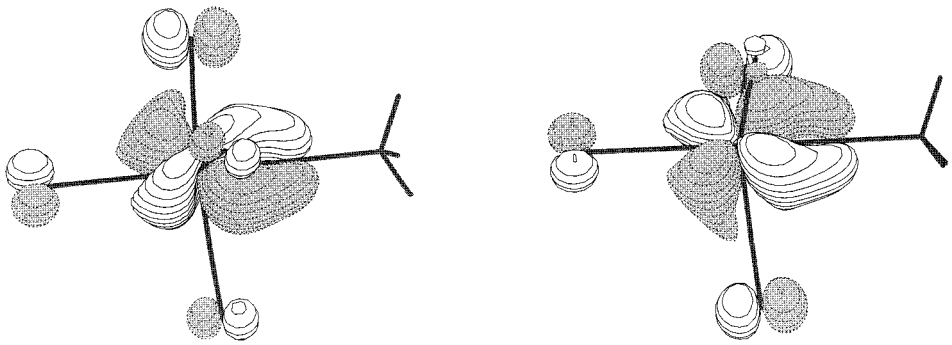

Figure 10. Three-dimensional drawings of the B ← Fe "back-bonding" molecular orbitals in $MeBFe(CO)_4$.

Table 10. Bond Energies, Energies of Complexation, Energy Decomposition and Reaction Energies for $RMFe(CO)_4$ Complexes[a]

	BE (M−Fe)	complexation energy[b]	E_{prep} (RM)	E_{prep} ($Fe(CO)_4$)	E_{prep} (total)	($E^\circ + E_{int}$)	reaction energy[d]
				(η^5-C_5H_5)$MFe(CO)_4$			
B	89.24 (−1512.07)[c]	−71.80 (1535.06)	4.59 (10.08)	12.85 (12.91)	17.44 (22.99)	−89.24 (1512.07)	−28.10
Al	67.22 (60.64)	−51.42 (−45.14)	3.92 (4.54)	11.88 (10.96)	15.79 (15.50)	−67.22 (−60.64)	−7.72 (−1.44)
Ga	51.03 (50.68)	−37.17 (−35.91)	3.72 (4.58)	10.15 (10.18)	13.86 (14.76)	−51.03 (−50.68)	6.54 (7.79)
In	(44.42)	(−31.34)	(3.11)	(9.96)	(13.07)	(−44.42)	(12.36)
				$MeMFe(CO)_4$			
B	108.87 (111.36)	−95.56 (−98.21)	0.07 (0.33)	13.24 (12.81)	13.31 (13.14)	−108.87 (−111.36)	−51.86 (−54.51)
Al	75.66 (71.89)	−63.09 (−59.97)	0.42 (0.57)	12.14 (11.35)	12.56 (11.91)	−75.66 (−71.89)	−19.39 (−16.27)
Ga	71.80 (69.98)	−59.87 (−57.96)	0.92 (1.12)	11.02 (10.90)	11.93 (12.02)	−71.80 (−69.98)	−16.16 (−14.25)
In	(65.69)	(−53.56)	(1.27)	(10.86)	(12.13)	(−65.69)	(−9.85)
				$(H_3Si)_2NBFe(CO)_4$			
	92.30	−79.55	0.21	12.54	12.75	−92.30	−35.85

[a] All data in kcal/mol. [b] RM + $Fe(CO)_4$ → $RMFe(CO)_4$. [c] Results for basis set B in parentheses. [d] RM + $Fe(CO)_5$ → $RMFe(CO)_4$ + CO.

stabilization energy resulting from the interaction of filled and unfilled orbitals on the reactants, E_{int}. The values of E_{rxn}, E_{prep}, and ($E^\circ + E_{int}$) are also listed in Table 10. Due to the minor geometrical changes that take place upon coordination, the preparation energies for the RM and $Fe(CO)_4$ fragments are predictably small—less than 5 kcal/mol for (η^5-C_5H_5)M, less than 2 kcal/mol for MeM, and approximately 10−12 kcal/mol for the $Fe(CO)_4$ fragment. Essentially, therefore, the entire reaction energy is attributable to the ($E^\circ + E_{int}$) term which, in turn, is dominated by the favorable interaction between the occupied donor orbital on RM and the LUMO on the $Fe(CO)_4$ fragment (the E° term is generally endothermic). A possible reason for the decreased exothermicity of the (η^5-C_5H_5)M complexes may be the expected increase in the E° term due to Pauli repulsion between the filled M π-orbitals and the appropriate Fe donor orbitals.

Although the primary strategy that was employed for the syntheses of the borane- and alanediyl complexes, (η^5-C_5Me_5)-$MFe(CO)_4$ (M = B, Al) involved the formal redox reaction of (η^5-C_5Me_5)MX_2 with $Na_2Fe(CO)_4$, Jutzi et al. obtained the analogous gallanediyl complex via the reaction of (η^5-C_5Me_5)-Ga with $Fe_2(CO)_9$ (which is essentially an $Fe(CO)_4$ fragment stabilized by $Fe(CO)_5$). The possibility of using the same approach, or alternatively the reaction of RM with $Fe(CO)_5$, to synthesize other $RMFe(CO)_4$ complexes (for M = B and Al) is suggested by the comparison of M−Fe and Fe−CO bond energies. The energy changes accompanying the following reaction (eq 3) are listed in Table 10. The calculated energies

$$RM + Fe(CO)_5 \rightarrow RMFe(CO)_4 + CO \qquad (3)$$

for all of the MeM ligand reactions are highly exothermic and therefore suggest that the direct reaction of these species with $Fe(CO)_5$ is a viable synthetic approach. An obvious potential problem, however, is that RM compounds typically form oligomers when R is an alkyl or silyl group which would disfavor the direct reaction with a transition metal carbonyl. It is somewhat interesting that the reaction of (η^5-C_5H_5)M with $Fe(CO)_5$ is predicted to be slightly endothermic for both Ga [ΔH: 6.54 (7.79) kcal/mol)] and In [ΔH: (12.36) kcal/mol)]. As stated above, the η^5-C_5Me_5 ligand forms complexes with shorter (M = Al, Ga), experimentally observed M−Fe bond distances and thus potentially stronger M−Fe bonds. Accordingly, the true reaction energies for all the (η^5-C_5Me_5)M ligands may be exothermic.[48]

With a view to gaining insight into the bonding in the recently reported amido-substituted boranediyl complexes, $(Me_3Si)_2NBM'L_n$ (M′ = Fe $(CO)_4$, $Cr(CO)_6$, $W(CO)_6$),[14] we have also carried out a DFT study of the model complex, $(H_3Si)_2NBFe(CO)_4$. The optimized geometry of $(H_3Si)_2NBFe(CO)_4$ is illustrated in Figure 6, and selected metrical parameters are listed in Table 7. Unfortunately, experimental structural data are not available for $(Me_3Si)_2NBFe(CO)_4$; hence direct comparison is not possible. Nevertheless, the GIAO calculated ^{11}B NMR shift for $(H_3Si)_2NBFe(CO)_4$ (73.1 ppm) is comparable to that obtained experimentally (88.2 ppm),[14] thus suggesting that the present model is reasonable. The most interesting features of the structure of $(H_3Si)_2NBFe(CO)_4$ concern the computed N−B and B−Fe bond distances. The N−B bond distance of 1.377 Å is slightly shorter than that computed for the free ligand (1.388 Å), thus implying the retention of the nitrogen−boron double bond and no B ← Fe back-bonding to that orbital. Interestingly, the calculated B−Fe bond distance for $(H_3Si)_2NBFe(CO)_4$ (1.835 Å) is identical to that calculated for (η^5-C_5H_5)-$BFe(CO)_4$, but much longer than that for $MeBFe(CO)_4$. Examination of a space-filling model of the $(H_3Si)_2NBFe(CO)_4$

(48) Other factors such as reaction temperature, steric effects, reaction kinetics, zero-point vibrational energies, solvent effects, and the loss of gaseous CO are undoubtedly important and could render the reaction thermodynamically favorable.

does not suggest that steric factors are dominant; hence, as in the case of (η^5-C_5H_5)BFe(CO)$_4$, the $(H_3Si)_2$NB ligand is acting primarily as a σ-donor and not as a π-acceptor. On the other hand, the metrical parameters for the Fe(CO)$_4$ fragment are intermediate between those for the iron tetracarbonyl fragments in the MeB and (η^5-C_5H_5)B complexes, which may be indicative of a modicum of B ← Fe back-bonding.

The charge distribution in $(H_3Si)_2$NBFe(CO)$_4$ is very similar to that in MeBFe(CO)$_4$. Moreover, as is the case for the other RBFe(CO)$_4$ complexes, the charge on boron increases by ~0.2, and that on the boranediyl substituent decreases by ~0.3 upon coordination of the boranediyl ligand. As expected, therefore, the $(H_3Si)_2$NB ligand is a net electron donor.

The orbital population analysis for $(H_3Si)_2$NBFe(CO)$_4$ is particularly informative because of the nondegeneracy of the boron p_x and p_y orbitals. The electron population of the boron p_y orbital, which is involved the N−B π-bonding, is 0.577 electrons and has increased from the value found in the free ligand (0.218 electrons). As in the case of (η^5-C_5H_5)BFe(CO)$_4$, this increase is caused by the increased charge on boron in the iron tetracarbonyl complex, which reduces the polarization of the N−B π-bond (vide infra) and increases the p_y orbital population. As discussed earlier, the boron p_y orbital population in the protonated ligand $(H_3Si)_2NBH^+$ (0.384) supports such an explanation but does not exclude the possibility of a slight back-bonding. More interesting is the population of the boron p_x orbital (0.429 electron) which is attributable to back-bonding from the Fe atom. Such a large increase in this orbital population suggests that the amido-substituted boranediyl is a reasonably strong electron acceptor, possibly due to the electronegativity of the amido substituent; however, the π-acceptor power of the $(H_3Si)_2$NB ligand is inferior to that of the MeB ligand. Interestingly, the computed B(p_x) orbital occupancy for $(H_3Si)_2NBH^+$ is 0.157 electron, which is is attributable to hyperconjugation from the N−Si bonds and might serve to reduce the p_x electron population caused by back-bonding.

Examination of the molecular orbitals of the $(H_3Si)_2$NBFe(CO)$_4$ complex reveals further details regarding the nature of the bonding. A selection of important orbitals is displayed in Figure 11. The σ-donor orbital [HOMO−5 (a′), energy: −0.3175 au] is of a shape and construction similar to those found for the other RMFe(CO)$_4$ complexes. Immediately above this donor orbital is the MO for the N−B π-bond [HOMO−4 (a′), energy: −0.30024] which clearly shows an increase in the magnitude of the wave function on the boron atom as compared to that of the free ligand. The lowest energy B ← Fe back-bonding orbital is the next highest in energy [HOMO−3 (a″), energy: −0.25391 au] and is very similar to the back-bonding MOs observed in MeBFe(CO)$_4$ complexes. All of the higher energy occupied MOs are primarily tetracarbonyl iron-based orbitals; however, the HOMO [(a″) energy: −0.20412 au] possesses considerable B−Fe π-antibonding character. The LUMO [(a″) energy: −0.25391 au] is primarily a boron-based orbital, again with a strong B−Fe π-antibonding component. The primary B−Fe σ-antibonding orbital [LUMO+4 (a′), energy: −0.04833 au] is located above the N−B π-antibonding MO [LUMO+2 (a′), energy: −0.06691 au]. Predictably, the molecular orbitals for $(H_3Si)_2$NBFe(CO)$_4$ in the plane of the boranediyl ligand are very similar to those for the methyl-substituted boranediyl analogue, whereas the N−B π-interaction dominates in the other plane.

Like the orbital and charge analysis data, the bond energies and energies of reaction calculated for $(H_3Si)_2$NBFe(CO)$_4$ fall between those for MeBFe(CO)$_4$ and (η^5-C_5H_5)BFe(CO)$_4$. The B−Fe bond energy for $(H_3Si)_2$NBFe(CO)$_4$ (92.30 kcal/mol) is much closer to that for (η^5-C_5H_5)BFe(CO)$_4$ (89.24 kcal/mol) than that for the MeBFe(CO)$_4$ (111.36 kcal/mol). Apparently, the more extensive back-bonding in $(H_3Si)_2$NBFe(CO)$_4$ does not strengthen the B−Fe bond appreciably which tends to explain the similarity in the B−Fe bond distance to that of (η^5-C_5H_5)BFe(CO)$_4$. Likewise, the energy of reaction for the formation of this complex from the $(H_3Si)_2$NB and Fe(CO)$_4$ components (−79.55 kcal/mol) is closer to that for (η^5-C_5H_5)-BFe(CO)$_4$ (−71.80 kcal/mol) than that for MeBFe(CO)$_4$ (−95.56 kcal/mol). The negligible differences in the structure of the $(H_3Si)_2$NB ligand in the free and complexed geometries implies a small preparation energy (0.21 kcal/mol) hence, as with the other RM species, the energy of reaction is dominated by the interaction of filled $(H_3Si)_2$NB orbitals with the acceptor orbitals

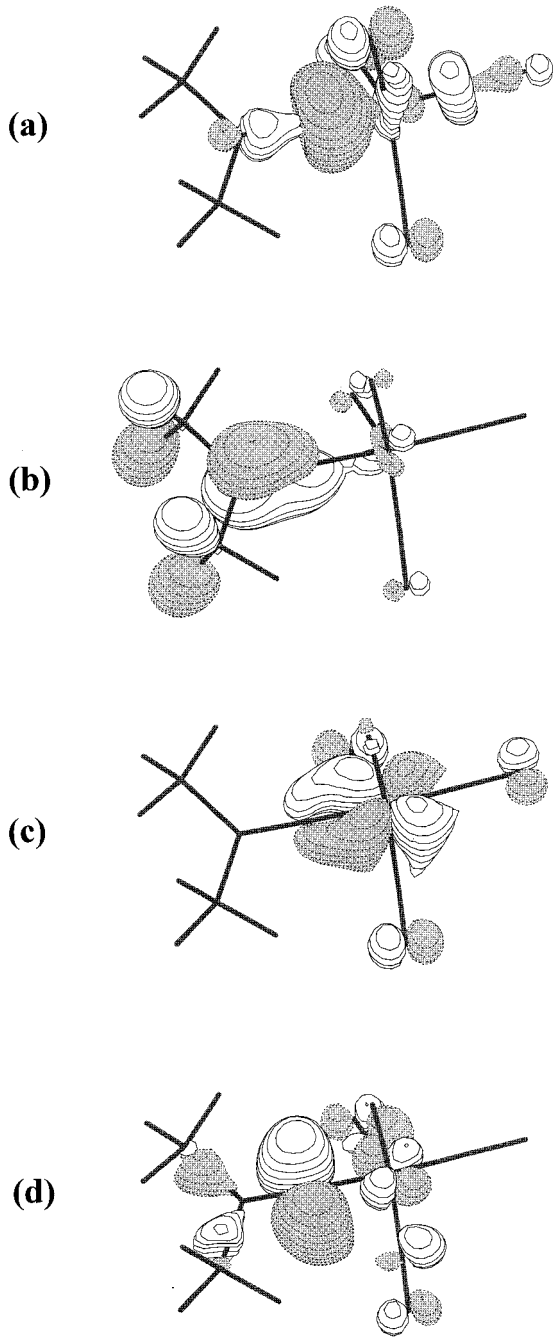

Figure 11. Three-dimensional depictions of selected molecular orbitals for $(H_3Si)_2$NBFe(CO)$_4$: (a) HOMO−5, (b) HOMO−4, (c) HOMO−3, (d) LUMO.

on the $Fe(CO)_4$ fragment. The reaction of $(H_3Si)_2NB$ with $Fe(CO)_5$ is predicted to be exothermic (−35.85 kcal/mol), a value which is intermediate between those for the MeB and (η^5-C_5H_5)B ligands.

In summary, the bulk of the data suggests that $(H_3Si)_2NB$ ligand is predominantly a two-electron donor with a slight capacity for π-acceptor bonding from the transition metal moiety. However, the back-bonding does not enhance the B−Fe bonding to any significant extent; hence, this ligand is best regarded as a vinylidene analogue with the predominant canonical form $(H_3Si)_2N{=}B{-}Fe(CO)_4$, as suggested previously.[2,21] In this light, drawing the amido-substituted boranediyl complex in the canonical form, $(H_3Si)_2N{=}B{=}W(CO)_5$, is clearly erroneous and not chemically meaningful. In particular, such a drawing contradicts the observation that the plane of the boranediyl ligand is canted at an angle of 37.2° from the closest plane containing two equatorial CO ligands. Moreover, a twisting of this magnitude diminishes the effective interaction of the metal d_{xz} and d_{yz} orbitals (in their standard orientation) with the empty boron p orbital on the boranediyl ligand.

Conclusions

Density functional calculations have been used to examine the bonding in free and $Fe(CO)_4$-complexed boranediyls and their heavier congeners. Regardless of the substituent R (R = η^5-C_5H_5, η^5-C_5Me_5, Me, $(H_3Si)_2NB$) the ground state of each RM fragment is a singlet, thus eliminating the double-bonded model **D**, which implies that the RM fragment bonds in a triplet ground state. In general, the univalent RM species are found to be two-electron donor ligands (bonding model **A**). In principle, the group RM species with non-π-donating R substituents could have some π-acceptor capability which is appropriate for metal−ligand back-bonding (bonding models **B** and **C**). However, evidence of such back-bonding has been found only in the case of the alkyl-substituted boranediyl complex, $MeBFe(CO)_4$ and not for the heavier group 13 analogues. In turn, this makes a bulky alkyl-substituted boranediyl transition metal carbonyl complex an attractive synthetic target. Overall, each boranediyl complex features a stronger M−Fe bond than any of its heavier congeners. From a theoretical standpoint, nearly all of the $RMFe(CO)_4$ complexes are potentially accessible by direct reaction of the isolated RM ligand with $Fe(CO)_5$; however, the oligomerization tendency of the monomeric RM species may tend to make this synthetic route less feasible.

The present results are not in agreement with the conclusion of Schnöckel et al.[20] that the bonding in (η^5-C_5Me_5)$AlFe(CO)_4$ is essentially ionic, i.e., the predominant canonical form is [(η^5-C_5Me_5)$Al]^{2+}[Fe(CO)_4]^{2+}$. We find no support for this ionic model for the following reasons: (i) the computed charges on the (η^5-C_5Me_5)Al and $Fe(CO)_4$ fragments are only ±0.75 (Table 9); (ii) there is unambiguous evidence for a bonding interaction between Al and Fe (see, for example, Figure 7 for analogous interactions of (η^5-C_5H_5)B or (η^5-C_5H_5)In with $Fe(CO)_4$); (iii) since $[Fe(CO)_4]^{2-}$ possesses a tetrahedral structure,[49] the experimentally observed[12] trigonal bipyramidal iron geometry would not be anticipated even if some counterion interaction were present; and (iv) as pointed out earlier, shortening of the average Al−C distance as (η^5-C_5Me_5)Al undergoes coordination to the $Fe(CO)_4$ fragment is expected on the basis of depopulation of the aluminum lone pair upon formation of the Al → Fe bond.

At the same time that the present work was submitted for publication, an article appeared[18] in which it was concluded that "there is a substantially higher degree of Ga ← Fe π back-bonding" in $C_6H_5GaFe(CO)_4$ than in (η^5-C_5H_5)$GaFe(CO)_4$. We have not performed calculations on $C_6H_5GaFe(CO)_4$ in the present work; however, in $MeGaFe(CO)_4$, where there is no indication of competitive π-donation from the organo substituent on gallium, we find no evidence for extensive Ga ← Fe back-donation. Frenking et al.[18] and Uhl et al.[6] also argue against the stability of species that feature only four valence electrons, thereby implying the necessity of oligomerization or group 13 element ← transition metal back-donation to render them isolable. However, such an argument is at variance with the isolation of one-coordinate indium derivative, InC_6H_3-2,6-$Trip_2$ (Trip = $-C_6H_2$-2,4,6-*i*-Pr_3), by Haubrich and Power.[8]

Acknowledgment. The authors are grateful to the National Science Foundation and the Robert A. Welch Foundation for generous financial support. We also thank Professor S. F. Martin for the use of an SGI Octane workstation.

Supporting Information Available: Tables of molecular orbital energies, triplet structural parameters, triplet spin densities, and some additional figures (PDF). This material is available free of charge via the Internet at http://pubs.acs.org.

JA992573L

(49) Teller, R. G.; Finke, R. G.; Collman, J. P.; Chin, H. B.; Bau, R. *J. Am. Chem. Soc.* **1977**, *99*, 1104.